Engineered Biochar as Gas Adsorbent

Duy Anh Khuong and Hong Nam Nguyen

Abstract From the 1100 s B.C to the present, biochar and adsorption technologies have been constantly evolving with a remarkable history. Biochar as a gas adsorbent is a biomass-derived material that has satisfactory properties for gas adsorption application. Since then, the mechanism, kinetics, and thermodynamics of gas adsorption have been investigated with the development of a series of novel models. Gas adsorption models are evaluated based on experimental adsorption isotherm, from which surface parameters of biochar can be derived. The surface and physicochemical characteristics of engineered biochar are ultimately determined by the type of the raw material and methods of char making including carbonization, physical activation, and chemical modification. Morphology, pH, total surface area, pore-volume, porosity, and surface functional groups are decisive factors for the gas adsorption capacity. Until now, biochar for gas adsorption is engineered for universal application to some gases such as CO_2, H_2S, CH_4, and N_2O, which are the main components of greenhouse gas emissions. Previous studies have shown the high efficiency of using engineered biochar as a gas adsorbent. However, it is still undeniable that this type of material still has certain limitations related to technical, economical, and environmental problems due to the knowledge gaps of mechanism, large-scale system, or regeneration process. Thus, in response to the current industrialization situation, it is mandatory to develop modern appropriate techniques to actualize the use of biochar as a gas adsorbent in the market.

Keywords Gas · Adsorption · Biochar · Modification · Structure · Adsorbent

D. A. Khuong (✉)
Department of Engineering, Kyushu Institute of technology, 1-1 Sensuicho, Tobata-ku, Kitakyushu 804-8550, Japan
e-mail: khuong.anh-duy591@mail.kyutech.jp

H. N. Nguyen
University of Science & Technology of Hanoi – Vietnam Academy of Science and Technology, 18 Hoang Quoc Viet, Cau Giay, Hanoi 100000, Vietnam

1   Introduction

1.1   *History of Gas Adsorption*

Gas adsorption is a surface mass transfer process, in which the gas molecules transfer and attach to the liquid or solid surfaces by physical or chemical forces (Artioli 2008). In reality, the natural adsorption phenomenon was coined and studied very early, with the first experiment being carried out by Gideon since 1100 B.C. century (Giles 1962). As reported, dew, otherwise known as the humidity of the air, was tested to be adsorbed on the fleece of wool fibers. Up to the fifteenth century, an architect named L. B. Alberti explained well about the adsorption of water, but it was not until 1773 that C. Scheele simultaneously J. Priestley and A. Fontana started to find a way to measure adsorption capacity systematically (Robens 1994).

The development of research in sorptometry technology has gone through a long history from 1100 BC to the end of the 20th century (Table 1), and is still ongoing at the present (Robens 1994; Kodama et al. 1987; Robens and Jayaweera 2014). Various methods to survey the adsorption have also been studied, such as hygrometry, thermogravimetry, calorimetry, thermoporometry, etc. However, sorptometry is the most preferred method because it gives high accuracy in the surface properties and adsorption capacity of a solid substance. Therefore, this chapter will emphasize the investigation of biochar as a gas adsorbent by sorptometry (gas adsorption apparatus).

1.2   *Origin of Biochar Applications*

Biochar, originally from charcoal, has been a commonly used material since ancient times. Despite the unknown first person who made charcoal, there are pieces of evidence as arrowheads fixed to their shaft with wood tar from the charring process, that were in use even as far back as 6000 years ago (Emrich 1985). The uses of charcoal are recorded to recover iron and metals from ores in Europe around 1100 BC, or for several different purposes in China since the Bronze Age (Chen et al. 2019). Over 2000 years ago, Amazonians in Brazil perhaps utilized biochar to fertilize their nutrient-poor tropical soils to feed a great agricultural civilization (King 2013). Through a lengthy historical period, modernization has led to the innovation of biochar applications from small-scale to industrial scale.

1.3   *Adsorbent—Application of Adsorption Technique on Biochar*

Over the decades, with the target to remove contaminants from gases economically and effectively, many kinds of adsorbents have been invented which are divided into

Table 1 Sorptometry development history until the 20th century

Investigation time	Method/Discovery	Inventor/Scientists
Around 1100 BC	First awareness of the adsorption (dew on fiber)	Gideon
1450	First gravimetric adsorption instrument	German cardinal Nicolaus Cusanus
End of 15th century	Inclination balances for atmospheric humidity measurement	Leonardo da Vinci
1773–1777	First recorded scientific adsorption measurements of water vapor (humid air) Used mercury to introduce a glowing charcoal piece into a reversed glass cylinder for adsorption measurement	Carl Scheele Priestley, Abbé Fontana
Around 18th century	Thin molecular layers on surfaces	Benjamin Franklin
1833	Thermogravimetry with 39 thermobalances for measuring water content of Chinese silk	Talabot
1881	Differ "adsorption at a surface" from "absorption in the interior"	Kayser, Du Bois Reymond
1886	First adsorption balance	Warburb and Ihmory
End of 19th century	First study about gas adsorption isotherms	Mitcherlich, Chappuis, Kayser
1912	First vacuum microbalance with electromagnetic compensation	Emich
1915	Thermobalance	Honda
1984	Measure standard weights in vacuum (high accuracy)	Japanese Researchers
1916–1918	Modern work on adsorption, Langmuir model	Langmuir
1938	BET theory	Brunauer, Emmet, Teller
1949	Application of gravimetric apparatus for surface area and pores investigation	van Nostrand
20th century	Volumetric apparatus (sorptometer) for simple gas, nitrogen adsorption isotherm	Chappuis, Emmett, Nelson and Eggertsen
1970–1999	The adsorption of gas (liquid-ike adsorbate) is calculated as a function of gas pressure at a fixed temperature	Sing, Gregg, Dabrowski, Rouquerol
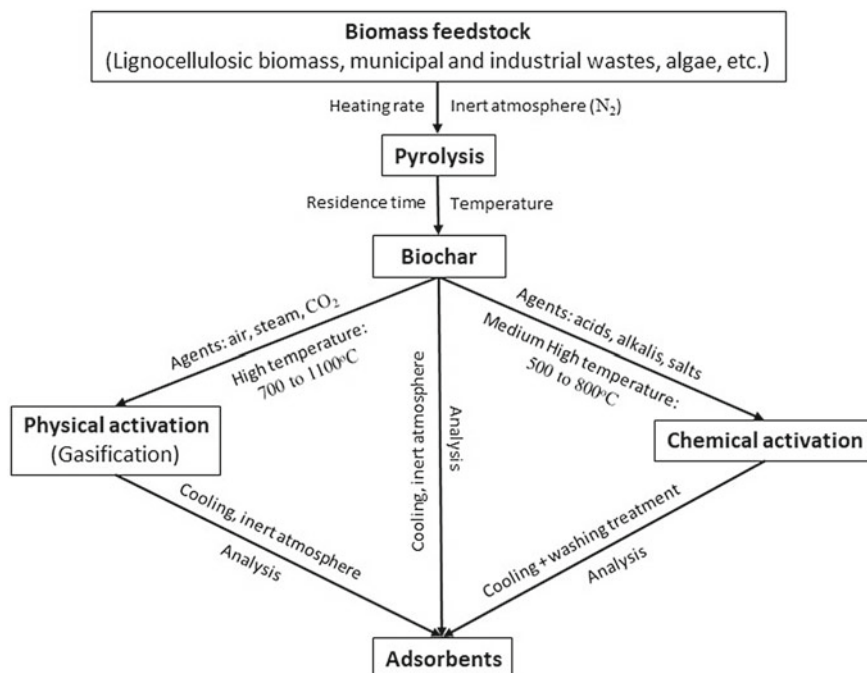
Fig. 1 The schematic of the procedure to make gas adsorbents from biomass

three main groups: carbon-based sorbents, silica-based sorbents, and metal–organic frameworks (MOF) (Bamdad et al. 2018). Nevertheless, carbon-based one, which is derived from biochar, is the most common due to its easy-to-find raw material, low cost, high efficiency and meets the demand for renewable materials (Fig. 1).

2 Principle of the Gas Sorption

2.1 Mechanism of Gas Adsorption and Desorption Processes

Adsorption is a phenomenon where gas molecules assemble on the adsorbent surface based on the mechanism of surface-based exothermic.

Otherwise, desorption is a reverse process of adsorption, in which molecules of the adsorbate are released from the adsorbent surface. The scheme of the adsorption/desorption process is represented in Fig. 2a. Depending on the interactions between the molecules of the gas compound and the surface of the adsorbent, adsorption could be defined as two types: "physisorption" and "chemisorption" (Rouquerol

(a)

(b)
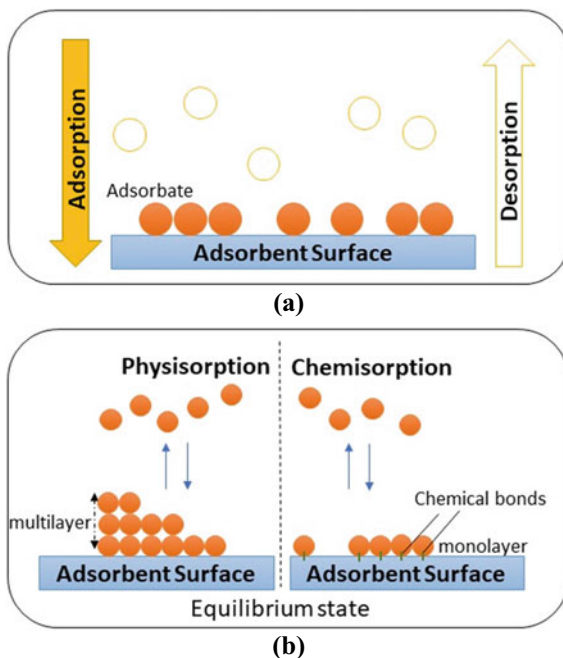
et al. 1999a). Physisorption or physical adsorption occurs by the physical weak forces including electrostatic interactions and Vander Waals force.

Physisorption can happen quickly, reversibly with no activation energy at low temperature, which usually forms multilayers of adsorbate molecules on the adsorbent surface. Meanwhile, chemisorption or chemical adsorption takes place slowly by the covalent bonds between the surface and molecules, irreversible with activation energy and high temperature required. It specifically involves the formation of the monolayer on the adsorbent surface (Dąbrowski 2001). Figure 2b shows the schematic explanation of the adsorption/desorption process and multi/monolayer of adsorbate molecules in the physical and chemical adsorption.

2.2 Isotherm of Gas Adsorption

International Union of Pure and Applied Chemistry (IUPAC) classified 6 types of adsorption isotherms (Fig. 3) (the gas adsorption) on the solid surface (Donohue and Aranovich 1998).

Type I is achieved from monomolecular gas adsorption on porous surfaces in a limited void volume. Meanwhile, unrestricted mono-multilayer adsorption without

Fig. 3 Different types of adsorption isotherm classified by IUPAC
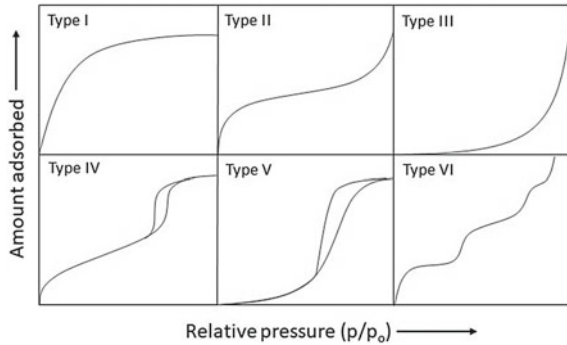
any saturation point is illustrated by the type II isotherm. It expresses the gas adsorption in the macroporous adsorbents. Type III isotherm indicates the weak interactions between adsorbent and gaseous adsorbate. Both Type II and Type III are for the nonporous or microporous adsorbent. Type IV isotherm has two parts: the first part represents mono-multilayer adsorption as Type II and the hysteresis loop is explained by capillary condensation in mesopores, which causes the progressive addition and withdrawal of adsorbate molecules on the adsorbent surface. Because Type V isotherm contains a hysteresis loop, this indicates the existence of mesopores. Type VI isotherm delineates the stepwise formation of multilayers of gas molecules on a uniform non-porous surface (Donohue and Aranovich 1998; Yahia et al. 2013).

Some popular models were invented to analyze the information about the gas–solid interface from the isotherm curves. A short explanation of these models is provided in Table 2.

2.3 Kinetics of Gas Adsorption

For a gas adsorption system, three common steps occurred during the process: (a) molecular mass transfer to the adsorbent surface, (b) internal molecular diffusion on the active sites, and finally (c) equilibrium state. In the case of uniform surfaces, the phenomenological kinetics of the sorption process is determined as the following equation (Zhdanov 2001):

$$\frac{d\theta}{dt} = k_a P - k_d \theta \tag{1}$$

where θ is the coverage, P is the sorption pressure, k_a and k_d are the rate constants representing the dependence between coverage and adsorption/desorption. The two parts of Eq. (1) $k_a P$ and $k_d \theta$ will be equal when the adsorption and desorption are at

Table 2 Description of some famous adsorption isotherm analysis models

Model	Equation	Assumptions	Reference
Langmuir	$\frac{C}{q} = \frac{1}{K_L q_{max}} + \frac{C}{q_{max}}$ C (mg L^{-1}): adsorbate molecules concentration at equilibrium state q (mg g^{-1}): the capacity of adsorbed molecules at any time q$_{max}$ (mg g^{-1}): the maximum adsorption capacity K$_L$ (L mg^{-1}): Langmuir constant	Adsorption at specific binding sites; all adsorption sites are similar; monolayer of molecules covers the adsorbent surface; no interaction at the gas–solid interface	(Langmuir 1918)
Freundlich	$q = K_F + C^{\frac{1}{n}}$ K$_F$ (mg g^{-1}): Freundlich exponent n: Freundlich constant	Heterogeneous multilayer adsorption	(Freundlich H 1911)
Temkin and Pyzhev	$q = \left(\frac{RT}{b}\right)\ln(AC)$ T (K): adsorption temperature R (8.314 Jmol^{-1} K^{-1}): ideal gas constant b (J mol^{-1}): Temkin constant A (L mg^{-1}): equilibrium adsorption constant—maximum adsorption energy	Adsorption heat decreases linear with the covering molecules layer	(TEMKIN 1940)
Harkins–Jura	$\left(\frac{1}{qe^2}\right) = \left(\frac{B_{HJ}}{A_{HJ}}\right) - \left(\frac{1}{A_{HJ}}\right)logC$ B$_{HJ}$ and A$_{HJ}$: Harkins–Jura constants	Multilayer adsorption process with heterogeneous pore distribution	(Harkins and Jura 1944)
Halsey	$t = 0.354\left[\frac{-5}{\ln(P/P_o)}\right]^{1/3}$ t: the thickness of adsorption layer on the nonporous silica surface	Same as Harkins–Jura	(Halsey 1948)
BET	$\frac{1}{X[(\frac{P_o}{P}-1)]} = \frac{1}{X_m C} + \frac{C_{BET}-1}{X_m C_{BET}}\left(\frac{P}{P_o}\right)$ X: the number of adsorbed gas molecules at a relative pressure P/P$_o$ X$_m$: the number of adsorbed gas molecules formed a monolayer C$_{BET}$: a heat adsorption second-parameter	Multilayer adsorption of the molecules to the adsorption surface	(Brunauer et al. 1938)
BJH	$log\frac{P}{P_o} = \frac{2\gamma V_M}{r RT}$ P/P$_o$: relative pressure in equilibrium γ: surface tension of liquid nitrogen V$_M$: molar volume of liquid nitrogen r (cm): radius of capillary	The pores shape is cylindrical; physisorption on the pore walls; capillary condensation inside the capillary volume	(Barrett et al. 1951)

Table 2 (continued)

Model	Equation	Assumptions	Reference
DFT	$N_{exp}\left(\frac{P}{P_o}\right) =$ $\int_{D_{min}}^{D_{max}} N_{QSDFT}\left(\frac{P}{P_o}, D\right) f(D) dD$ $N_{exp}(P/P_o)$: experimental adsorption isotherm (number of moles adsorbed at a pressure P) $N_{QSDFT}(P/P_o, D)$: theoretical isotherm in pores series D: pore size (width) f(D): pore size distribution function D_{min} and D_{max}: minimum and maxmium pore size	Pores are the slit-shaped type	(Seaton et al. 1989; Landers et al. 2013)

equilibrium. Another elucidation of this phenomenon is the same chemical potential of adsorbed and gas-phase particles. However, to access in-depth the adsorption kinetics on the non-uniform surface, it is necessary to apply some adsorption systematic models. The first-known important model is the pseudo-first-order model of Lagergren (1898) with the given equation:

$$\frac{dq_t}{dt} = k_1(q_o - q_t) \tag{2}$$

where q_t is the gas adsorbed amount (mg g^{-1}) at any time t (min), q_o is adsorbed amount at equilibrium, and k_1 is the rate constant of the first-order process (min^{-1}). Following this model, the adsorption happens only on the specific site of the adsorbent surface, with no interaction between gas molecules and surface, the adsorption energy is independent with the molecular layer formation and the adsorption rate is managed by the Eq. (2).

The developed version from the first model is pseudo-second-order (Ho and McKay 1999), which is exposed by Eq. (3):

$$\frac{dq_t}{dt} = k_2(q_o - q_t)^2 \tag{3}$$

This model is supposed to give a great correlation of the experimental data from some systems, though the assumptions made are identical to the previous version except for the model rate (k_2).

Besides, the intraparticle diffusion model proposed by Weber and Morris (1963) is also widely applied for describing the adsorption process, where the diffusion of the adsorbate on the adsorbent surface is the rate-limiting step.

$$q_t = k_3 t^{0.5} \tag{4}$$

where k_3 is the intraparticle diffusion constant rate.

2.4 Thermodynamics of Gas Adsorption

The understanding of the thermodynamics principle was enhanced thanks to the study of Rouquerol et al. (1999b, 2014) about the adsorption at the gas–solid interface. Their thermodynamic quantities investigation is highly effective to process as well as interpret the experimental isotherms and data, especially the effect of temperature on the adsorption process. Based on some thermodynamic parameters as enthalpy, Gibbs energy, and entropy, the behavior sorption process can be forecasted. The transformed Gibbs energy (G), which is also called the thermodynamic potential of adsorption at equilibrium, is calculated as:

$$G = F + pV + \gamma A \tag{5}$$

where F is Helmholtz energy, p, V are adsorption pressure and volume of adsorbed gas respectively, γ is surface tension and A is the solid adsorbent's surface area. One usual method to excess differential enthalpies ($\Delta_{ads}\dot{h}$) from the adsorption isothermal data is the Isosteric Method.

$$\Delta_{ads}\dot{h} = -\frac{RT_1 T_2}{T_2 - T_1} ln\frac{p_2}{p_1} \tag{6}$$

By measuring a series of adsorption isotherms at different temperatures and applying Eq. (6), the differential enthalpy or isosteric heat of adsorption would be determined as a function of equilibrium pressure P_1, P_2, and temperature T_1, T_2. The differential standard entropy ($\Delta_{ads}\dot{s}$) can also be inferred as:

$$\Delta_{ads}\dot{s} = \Delta_{ads}\dot{h} - Rln[p] \tag{7}$$

For determining the isosteric heat of adsorption, some other methods were also proposed as gas adsorption calorimetry, immersion calorimetry, and chromatographic methods. The characteristics of the adsorption process are defined by the differential Gibbs energy and enthalpies. The adsorption process is considered to be spontaneous when the ΔG value is negative and be endothermic when the $\Delta_{ads}\dot{h}$ value is positive (Kecili and Hussain 2018).

3   Changing Biochar Properties by Modification

The microporosity of biochars was demonstrated to be promoted and dominated by CO_2 activation, while steam activation helps develop the meso- and macroporous structure as well as a larger pore size distribution. However, due to the intimate relationship between ascending porosity and descending degree of burned-off char, the industrial process for modified biochar would have a limitation for a yield of about 40 wt% activation (Rodríguez-Reinoso 2001). As reported, steam activation nearly doubled the surface area of biochar produced from *Miscanthus* while degrading functional groups, which led to weakening the polarity (Shim et al. 2015). The surface area and pore volume of biochar derived from teak sawdust by vacuum pyrolysis method were sanitated, from approximately 611 m^2 g^{-1} and 0.27 cm^3 g^{-1} to 1150 m^2 g^{-1} and 0.37 cm^3 g^{-1}, by steam activation (Ismadji et al. 2005). In a very recent study, the bamboo residue char had a dominant microporous structure with a specific area of 2150 m^2 g^{-1} after being activated by CO_2 gas (Khuong et al. 2021a). By air oxidation, a great amount of oxygenated functional groups as carboxylic, lactonic, and phenolic were generated on the surface of biochar (Bardestani and Kaliaguine 2018). However, air activation at the high temperature has a challenge with the controlling step due to its sensitivity and high reactivity with carbon, which can lead to burn-off char, a high percentage of macropore but poor porosity (Sajjadi et al. 2019). Physical activation deforms the surface structure of biochar differently from using the alternative pyrolysis method to modify the char.

Figure 4 shows the morphologies at the same scale ($\times$1000) of the residue bamboo-derived pyrolyzed at 800 °C, pyrolyzed at 900 °C, and activated by CO_2 at 800 °C for 6 h. As can be seen, the increase of 100 °C in pyrolysis stretched the shape or shattered the edge boundary between macropores, instead, CO_2 activation disrupted most of the capillary structure.

Depending on the selected category of agents, the single-step activation or two-step activation will have certain beneficial effects. For H_3PO_4 activation, a single-step process was demonstrated to be higher effective, whereas the char products were more amorphous, possessing an applicable porous structure with high adsorption capacity (Oginni et al. 2019). A two-step activation was proved to be more advantageous for KOH activation, which modified biochar derived from rice straw in a superior way, high BET specific area, and low ash content (Basta et al. 2009). In the research of activated carbon produced from seed shells, $ZnCl_2$ was considered to be a more effective agent than H_3PO_4 due to its higher adsorption capacity product despite a lower yield (Nsi et al. 2016). Apart from a dependency on activation methods and activating agent types, the impregnation ratio between the material and agent, and the concentration of agent also extremely impacts the growth of porosity. The previous investigation showed that the increment of the concentration as well as the ratio of H_3PO_4 or $ZnCl_2$ led to enlarging pores and surface area, for instance, the BET surface area of activated biochar from *Oreganum* stalks increased from 497 m^2 g^{-1} to 730 m^2 g^{-1} when the H_3PO_4 concentration raised from 40 wt.% to 120 wt.% (Timur et al. 2006). Additionally, some other chemical modification methods such as using
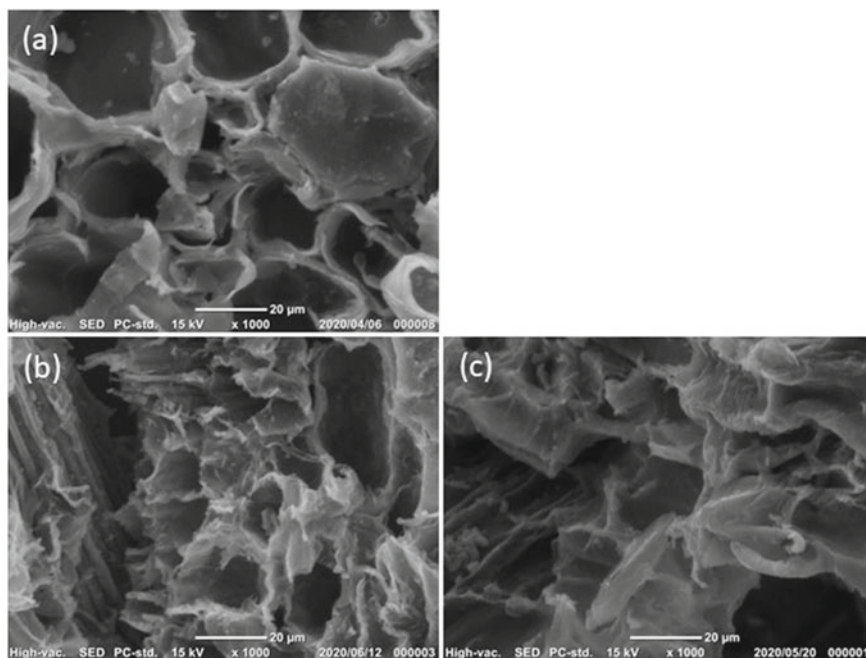
Fig. 4 The morphologies measured by SEM technique of the samples (**a**) pyrolyzed at 800 °C; (**b**) pyrolyzed at 900 °C; (**c**) CO_2 activated at 900 °C

salts, ammonium hydroxide (NH_4OH), ammonia (NH_3), hydroxylamine (NH_2OH), carbamide—urea ($CO(NH_2)_2$), iron, amines, triethylenetetramine—TETA, etc., with heat treatment are applied in biochar to functionalize the surface properties for higher uptake capacity, especially CO_2 uptake (Petrovic et al. 2021). The physical activation allows the narrow pore size distributions with low packing densities, while the chemical process grants the biochar with lower weight loss, high packing densities, and elevated mesoporosity (Prauchner and Rodríguez-Reinoso 2012).

4 Studies of Engineered Biochar as Gas Adsorbent

Over the past few decades, the gas adsorbents derived from biochar were employed, modified, and developed due to the rapid development of society that required clean gas application for environmental regulations (Menéndez-Díaz and Martín-Gullón 2006). Except for nitrogen (N_2), which is used majorly for discovering the porous parameters of adsorbents, the main adsorbate gases being studied at present are acidic gases such as CO_2, CH_4, H_2S, N_2O. Each adsorbate has a different adsorption mechanism on the surface of the adsorbent.

4.1 CO$_2$ Adsorbents

As aforesaid, the capacity of adsorption compromises with the adsorption conditions as well as the characteristics of biochar-derived adsorbent, which is largely determined by the raw material and the method of modification. Table 3 mentions the CO$_2$ uptakes recorded from multiple reports that used various materials and techniques.

The activated vine shoots sample in Table 3 is a typical case for the temperature and atmosphere dependence of adsorption capability, that is, an increase in temperature and decrease in pressure led to the decrement in CO$_2$ uptake. Another study considered that the physisorption adjusted the CO$_2$ adsorption of biochar, whereas physical adsorption generates 5 to 40 kJ mol^{-1} and chemical adsorption produced 40 to 800 kJ mol^{-1} of adsorption heat (Creamer 2017). From the table, it is clear that the CO$_2$ capture ability is governed by the unique structure and surface properties of modified biochar. Sawdust without activation or modification has the CO$_2$ uptake of only 18 mg g^{-1} at 25 °C and 20.7 bar, and this number increased to 44.8 mg g^{-1} at 30 °C when the material was modified by monoethanolamine. Cellulose fiber activated by steam could access higher CO$_2$ capacity than bamboo activated by CO$_2$ at the same adsorption condition, although the specific surface area of activated cellulose was lower than activated bamboo. Other samples including Eucalyptus wood, Rambutan peel, African palm shell, sea mango, Miscanthus yielded very promising CO$_2$ adsorption results. These samples were especially surface-functionalized with different methods to improve the CO$_2$ uptake.

The presence of basic functional groups has helped to retain the CO$_2$ gas molecules in pores instead of letting them slide out when approaching equilibrium. Some nitrogen-containing functional groups as amide, pyridinic, imide, pyrrolic, lactam groups, can be contributed to the biochar surface by N-containing reagents as ammonia, amines, nitric acid, or any N-containing precursors (Dissanayake et al. 2020). It was also demonstrated that the CO$_2$ uptake is attributed to many factors: surface area, nitrogenous groups, pore structure, size, micropore surface area, and volume (Khandaker et al. 2020). Hence, the mechanism of CO$_2$ adsorption should be evaluated according to the experimental case.

4.2 Other Gas Adsorbents

Recently hydrogen sulfide (H$_2$S) and methane (CH$_4$) have also been studied. To investigate the H$_2$S or CH$_4$ adsorption capacity of adsorbents, the breakthrough curves must be defined, constructed and analyzed. A breakthrough curve is known as a technical plot that shows the correlation between the concentration of adsorbate and the testing time interval. The adsorbate amount is measured through the capacity of the bed of the adsorbent, where the effluent stream of a mixture of fluid (air and

Table 3 Some reported biochar modification methods and their CO_2 adsorption capacity

Raw material	Modification methods	S_{BET} (m^2 g^{-1})	Adsorption condition	CO_2 uptake	Reference
Sawdust	Pyrolysis at 650 °C; nil	~ 200	25 °C–300 psi (20.7 bar)	18 mg g^{-1}	Ghani and Silva (2014)
Vine shoots	Pyrolysis at 600 °C; KOH activation at 700 °C	1671	25 °C–1 bar 0 °C–1 bar 0 °C–15 kPa	2.46 mmol g^{-1} 5.40 mmol g^{-1} 2.25 mmol g^{-1}	Manyà et al. (2018)
Cellulose fiber	Pre-pyrolysis at 200 °C; steam activation at 800 °C	863	25 °C–1 bar	3.78 mol g^{-1}	Heo and Park (2015)
Bamboo	Pyrolysis and CO_2 activation at 800 °C	952	25 °C–1 bar	3.4 mmol g^{-1}	Khuong et al. (2021b)
Eucalyptus Wood	H_3PO_4 activation at 450 °C; NH_3 modification at 800 °C	2079	30 °C–1 bar	3.22 mmol g^{-1}	Heidari et al. (2014)
Rambutan peel	Pyrolysis at 900 °C; $Mg(NO_3)_2$ modification at 800 °C	~ 505	30°C–75 ml min^{-1} CO_2	75.58 mg g^{-1}	Zubbri et al. (2020)
African palm shell	$CaCl_2$, H_3PO_4 and CO_2 combination activation at 900 °C; NH_4OH modification at 75 °C	634	0 °C–1 bar	333 mg g^{-1}	Giraldo et al. (2020)
Sea mango	Pyrolysis at 200°C; H_3PO_4 activation at 500 °C (absence of any gases); deep eutectic solvent modification	~ 436	15% CO_2 in 5 ml/min	9.685 mg g^{-1}	Zulkurnai et al. (2017)
Miscanthus	Pyrolysis at 700 °C, low-frequency ultrasound and TEPA activation; EDC and HOBt functionalization	532	70 °C–0.1 atm	2.89 mmol g^{-1}	Chatterjee et al. (2020)
Cottonwood	Metal (Al) oxyhydroxide composites modification at 600 °C	367	25 °C–50 ml min^{-1} CO_2	71.05 mg g^{-1}	Creamer et al. (2016)
Sawdust	Pyrolysis at 850 °C, Monoethanolamine (MEA) modification	3.17	30 °C–100 ml min^{-1} CO_2 70 °C–100 ml min^{-1} CO_2	44.8 mg g^{-1} 25.2 mg g^{-1}	Madzaki et al. (2016)

vapor in this case) enters until reaching the saturation state (Marsh and Rodríguez-Reinoso 2006). The mechanism of the H_2S adsorption is based on several processes with equation expressed as follows (Shang et al. 2013):

H_2S gas molecules adsorb on the adsorbent surface.

$$H_2S_{gas} \xrightarrow{K_H} H_2S_{ads} \qquad \text{(Reaction 8)}$$

H_2S dissolves in a water film made from the moisture of the adsorbent.

$$H_2S_{ads} \xrightarrow{K_S} H_2S_{ads-liq} \qquad \text{(Reaction 9)}$$

H_2S adsorbate dissociates in the water film.

$$H_2S_{ads-liq} \xrightarrow{K_a} HS^-_{ads} + H^+ \qquad \text{(Reaction 10)}$$

Anion element of dissociation reacts with adsorbed oxygen (O_2) and forms sulfur (S) or sulfur dioxide (SO_2).

$$HS^-_{ads} + O^*_{ads} \xrightarrow{K_{R1}} S_{ads} + OH^- \qquad \text{(Reaction 11)}$$

$$HS^-_{ads} + 3O^*_{ads} \xrightarrow{K_{R2}} SO_{2ads} + OH^- \qquad \text{(Reaction 12)}$$
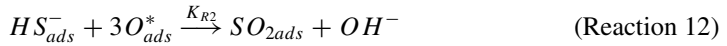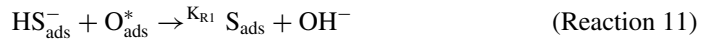
SO_2 is oxidized to H_2SO_4 in the water created from the adsorption.

$$H^+ + OH^- \rightarrow H_2O \qquad \text{(Reaction 13)}$$

$$SO_{2ads} + O^*_{ads} + H_2O_{ads} \xrightarrow{K_{R3}} H_2SO_{4ads} \qquad \text{(Reaction 14)}$$

The *gas, ads, ads-liq* are noted for the phases of elements, for instance, H_2S_{gas} corresponds to H_2S in the gas phase, $H_2S_{ads-liq}$ or H_2S_{ads} stands for H_2S in the liquid phase or adsorbed phase. K_H, K_S, and K_a are the equilibrium constants for the adsorption process, gas solubility process, and dissociation process, respectively. K_{R1}, K_{R2}, and K_{R3} are the surface reaction constants. There are some individual investigations on H_2S, with 3 case studies listed in Table 4. These studies indicated that the surface characteristics and pH of biochar rule the mechanism as well as the capacity of the adsorption. The rational use of the raw material and modification methods have brought potential results. Rice husk char achieved a high breakthrough capacity of 382.7 mg g^{-1} in an H_2S environment. Each gram of Maple sawdust with Fe-impregnation can adsorb 15.2 mg of H_2S in a biogas flow. In addition to agriculture residue, activated food waste and sludge could also adsorb a great amount of H_2S, 66.6 mg g^{-1} in gas matrices.

Table 4 Some approach for engineered biochar as H₂S gas adsorbent

Raw material	Modification methods	pH	Adsorption condition	Breakthrough capacity (mg g⁻¹)	Reference
Camphor	Pyrolysis at 400 °C; nil	9.55	Room temperature–40 ml min⁻¹ H₂S	109.3	Shang et al. (2013)
Rice husk		10.56		382.7	
Bamboo		10.21		336.7	
Corn stover	Pyrolysis at 500 °C	10.2	Room temperature–100 mL min⁻¹ biogas	0.5	Choudhury and Lansing (2021)
	Pyrolysis at 500 °C and Fe-impregnated	9.10		1.5	
Maple sawdust	Pyrolysis at 500 °C	2.80		2.0	
	Pyrolysis at 500 °C and Fe-impregnated	6.97		15.2	
Wood pallet	Pyrolysis at 700 °C	7.3	Room temperature–0.18 L min⁻¹ gas matrices	0.04	Hervy et al. (2018)
	Pyrolysis at 700 °C; Oxygenation at 280ᴾᶜ	7.6		1.81	
	Pyrolysis at 700 °C; steam activation at 850 °C	9.0		12.92	
Food waste and coagulation flocculation sludge	Pyrolysis at 700 °C	9.6		0.22	
	Pyrolysis at 700 °C; Oxygenation at 280ᴾᶜ	9.6		0.12	
	Pyrolysis at 700 °C; steam activation at 850 °C	9.8		66.60	

Different from H_2S, the adsorption mechanism of CH_4 is self-diffusion, in which the isosteric heat ranges from 8.715 to 11.746 kJ mol^{-1} at 233.15–363.15 K (40 °C– 90 °C) (Wang et al. 2020). Sadasivam and Reddy. (2013, 2014, 2015) applied batch and column adsorption testing methods on biochar derived from woody biomass to explore the transport and adsorption of methane collected in landfills. The adsorption capacity of activated biochar from a mixture of pine and fur wood was found to be up to 3333.3 mL kg^{-1} at 10% CH_4 headspace concentration (Sadasivam and Reddy 2013). At the dry condition, the biochar derived from a type of wood waste (CE-WP1) had a calculated value of CH_4 adsorption capacity 0.21 mol kg^{-1} from the Langmuir model. This value decreased to 0.11 mol kg^{-1}, still higher than that of granular activated carbon (0.06 mol kg^{-1}) when the corresponding water holding capacity was 25% at room temperature (Sadasivam and Reddy 2015). Wood pellet biochar produced from pyrolysis 500 °C had a much higher extent of methane diffusion than that of granular activated carbon (Sadasivam and Reddy 2014).

Likewise, the simultaneous adsorption of gaseous adsorbates is crucial for engineering effective biochar. The selectivity of CO_2, H_2S, and CH_4 gases during the adsorption has been surveyed on some biochar derived from perilla, oak, and soybean stover (Sethupathi et al. 2017). For biochar mentioned in the literature, when adsorbing singular gas, CO_2 was the most adsorbed with adsorption capacity up to 2.312 mmol g^{-1}. Nonetheless, when simultaneous adsorption occurred, H_2S dominated over CO_2 adsorbate, and CH_4 was barely adsorbed. This phenomenon can be explained by the fact that the small CO_2 and H_2S molecules with 3.3 Å and 3.6 Å kinetic diameters, respectively, permeate all the porous structures, even in ultra-micropores, which prevents the CH_4 molecules with the large kinetic diameter of 3,8 Å from being adsorbed on the adsorbent surface (Cui et al. 2004; Scholes et al. 2010; JALON 2017). The breakthrough capacities of H_2S and CO_2 were recorded as 0.208 mmol g^{-1} and 0.126 mmol g^{-1} respectively in the 700 °C-pyrolyzed perilla. It was also disclosed that the biochar from perilla possessed a high adsorption capacity of H_2S and CO_2, which was followed by soybean stover and oak biochar (Sethupathi et al. 2017).

Different from the above mentioned gases, nitrous oxide (N_2O) exists in soils and oceans as a byproduct of nitrification and denitrification ((Machida et al. 1995). Therefore, the application of N_2O adsorption is in biochar-amended soil to suppress its emission in the atmosphere (Solaiman and Anawar 2015). The mechanism of N_2O removal by biochar can be explained by the "electron shuttle", a redox system that easily switches between states and facilitates electron transmissions to microorganisms (Cayuela et al. 2013). It is also noted that the biochar N_2O adsorption capacity is strongly influenced by soil texture, soil pH, and the chemical form of N-fertilizer (Cayuela et al. 2014). The physicochemical treated pecan shell, maple wood, and pinewood could adsorb 4.3 - 21 mmol N_2O per kg, while Lockwood soil or peat could adsorb only 0.13 mmol N_2O per kg at the same low relative pressure condition (Xiao et al. 2018). By adding hardwood-derived biochar in sandy loam soil at a rate of 28 Mg ha^{-1}, N_2O emissions were suppressed 91% of the total amount (Rittl et al. 2021).

5   Limitations

Biochar as gas adsorbent is an attractive topic that is broadly approached in recent years, especially for CO_2 capture application. Biochar is an eco-friendly and low cost product (10 times cheaper than other CO_2 adsorbents) (Chatterjee et al. 2018). However, biochar-based gas adsorbents are still constrained by numerous challenges related to technical, economical, and environmental aspects.

There are many studies on the enhancement of gas adsorption capacity after biochar modification, however, the stability and durability of products have not been clarified for the long-term assessment (Dissanayake et al. 2020). Most studies concentrated only on certain gases or a combination of predetermined gases. Nonetheless, for greenhouse gas emissions (GHG) containing multiple gaseous agents, the removal mechanism is indeed complicated (Solaiman and Anawar 2015), which requires a comprehensive understanding of the effect of each gas on one other during the adsorption process. Besides, the adsorptive characteristics of biochar can be degraded during long-term cyclic sorption, which should be taken into account in the technical issues for biochar production (Zhelezova et al. 2017). So far, the data related to the operation in the continuous flow system as well as the regeneration capacity of modified biochar has not been elucidated (Rosales et al. 2017).

In the case of the economical aspect, Gwenzi et al. (2021) suggested some present knowledge gaps including the lack of studies on the applications of biochar as a gas adsorbent on a large-scale or industrial scale, the scarcity of socio-economic feasibility research, and the competition from existing biochar production technologies. Perhaps, the treatment process of modified biochar is not as cost-effective as bio-oil technology, which also utilized bio-waste or biomass as the raw material.

Although biochar supports the mitigation of GHG emissions, its production produces a relatively large quantity of polycyclic aromatic hydrocarbons (PAHs) and dioxins that cause human and ecological risks (Hale et al. 2012). Furthermore, the amended biochar from wastewater sludge or possibly other residues might accommodate a high level of heavy metal as Zn, Pb, Ni, Cu, Cd (Hossain et al. 2011), which raises difficulties of spent biochar disposal. Without proper control and treatment, the biochar may also migrate in soil that induces negative influences on the ecosystem as well as human lives (Genesio et al. 2016).

In addition to the above rationale, policy and regulatory framework for enhancing biochar as gas adsorbent is also a challenge that needs to be dealt with (Gwenzi et al. 2021). Due to a lack of understanding of technological components, setting development policies will be a big question for future research.

6 Conclusions and Future Prospects

Up to now, a number of studies on the gas adsorption application of biochar have been accomplished and yielded positive results. The physicochemical properties and porous structure of biochar including pH, constituent elements, porosity, morphology, and surface functional groups are the decisive factors for gas adsorption performance. Therefore, to ameliorate the gas adsorption capacity, the characteristics of char products from pyrolysis should be boosted by physical and chemical modifications. Previous findings of modified biochar have shown its superiority in adsorbing gases in the environment, helping to mitigate GHGs, which include mainly CO_2, H_2S, CH_4, N_2O. However, the lack of knowledge in many aspects has posed plenty of challenges for bringing biochar into the potential market of gas adsorption technologies. With the current increasing rate of gaseous pollutants from burning fuels, greenhouse gas emissions, and industrial constructions, novel techniques for gas adsorption application on biochar should be focused on the development of the capacity, regeneration, and reuse features for the industrial scale.

Based on the challenges mentioned above, it is necessary to establish certain strategies to solve those difficulties. Conducting research to solve the technical problems that include the gas mixture adsorption and regenerative long-term techniques should be promoted. Besides, studies on other technologies related to biomass also need to be done, especially economic analysis, to find ways to bring biochar as a gas adsorbent to consumption in the actual market. Above all, a complete database on biochar production and adsorption capacity of a combination of multiple gases should be created to maximize char performance, minimize environmental problems, and set forth new appropriate policies.

References

Artioli Y (2008) Adsorption. In: Jørgensen SE, Fath BD (eds.) Encyclopedia of ecology. Academic Press, Oxford, pp 60–65

Bamdad H, Hawboldt K, MacQuarrie S (2018) A review on common adsorbents for acid gases removal: focus on biochar. Renew Sustain Energy Rev 81:1705–1720

Bardestani R, Kaliaguine S (2018) Steam activation and mild air oxidation of vacuum pyrolysis biochar. Biomass Bioenerg 108:101–112

Barrett EP, Joyner LG, Halenda PP (1951) The determination of pore volume and area distributions in porous substances. I. computations from nitrogen isotherms. J Am Chem Soc 73(1):373–380

Basta AH, Fierro V, El-Saied H, Celzard A (2009) 2-Steps KOH activation of rice straw: an efficient method for preparing high-performance activated carbons. Biores Technol 100(17):3941–3947

Brunauer S, Emmett PH, Teller E (1938) Adsorption of gases in multimolecular layers. J Am Chem Soc 60(2):309–319

Creamer AE, Gao B, Wang S (2016) Carbon dioxide capture using various metal oxyhydroxide–biochar composites. Chem Eng J 283:826–832

Creamer AE (2017) Carbon dioxide capture with pyrogenic carbon-based materials. https://ufdc.ufl.edu/UFE0050961/00001, Accessed 25 May 2021

Cayuela ML, Sánchez-Monedero MA, Roig A, Hanley K, Enders A, Lehmann J (2013) Biochar and denitrification in soils: when, how much and why does biochar reduce N 2 O emissions? Sci Rep 3(1):1732

Cayuela ML, van Zwieten L, Singh BP, Jeffery S, Roig A, Sánchez-Monedero MA (2014) Biochar's role in mitigating soil nitrous oxide emissions: a review and meta-analysis. Agr Ecosyst Environ 191:5–16

Chatterjee R, Sajjadi B, Chen W-Y, Mattern DL, Hammer N, Raman V, Dorris A (2020) Effect of pyrolysis temperature on physicochemical properties and acoustic-based amination of biochar for efficient CO2 adsorption. Front Energy Res 8:85

Chatterjee R, Sajjadi B, Mattern D, Chen W-Y, Zubatiuk (Klimenko) T, Leszczynska D, Leszczynski J, Egiebor N, Hammer N (2018) Ultrasound cavitation intensified amine functionalization: a feasible strategy for enhancing CO2 capture capacity of biochar. Fuel 225:287–298

Chen W, Meng J, Han X, Lan Y, Zhang W (2019) Past, present, and future of biochar. Biochar 1(1):75–87

Choudhury A, Lansing S (2021) Adsorption of hydrogen sulfide in biogas using a novel iron-impregnated biochar scrubbing system. J Environ Chem Eng 9(1):104837

Cui X, Bustin RM, Dipple G (2004) Selective transport of CO2, CH4, and N2 in coals: insights from modeling of experimental gas adsorption data. Fuel 83(3):293–303

Dąbrowski A (2001) Adsorption—from theory to practice. Adv Coll Interface Sci 93(1):135–224

Dissanayake PD, You S, Igalavithana AD, Xia Y, Bhatnagar A, Gupta S, Kua HW, Kim S, Kwon J-H, Tsang DCW, Ok YS (2020) Biochar-based adsorbents for carbon dioxide capture: a critical review. Renew Sustain Energy Rev 119:109582

Donohue MD, Aranovich GL (1998) Classification of Gibbs adsorption isotherms. Adv Coll Interface Sci 76–77:137–152

Rosales E, Meijide J, Pazos M, Sanromán MA (2017) Challenges and recent advances in biochar as low-cost biosorbent: from batch assays to continuous-flow systems. Bioresour Technol 246:176–192

Emrich W (1985) History and fundamentals of the charcoal process. In: Emrich W (ed) Handbook of charcoal making: the traditional and industrial methods. Springer, Netherlands, Dordrecht, pp 1–18

Genesio L, Vaccari FP, Miglietta F (2016) Black carbon aerosol from biochar threats its negative emission potential. Glob Change Biol 22(7):2313–2314

Ghani W, Silva G (2014) Sawdust-derived biochar: characterization and CO2 adsorption/desorption Study. J Appl Sci 14:1450–1454

Giles CH (1962) Gideon's fleece tests: the earliest recorded vapor phase adsorption experiment? J Chem Educ 39(11):584

Giraldo L, Vargas DP, Moreno-Piraján JC (2020) Study of CO2 adsorption on chemically modified activated carbon with nitric acid and ammonium aqueous. Front Chem 8:543452

Gwenzi W, Chaukura N, Wenga T, Mtisi M (2021) Biochars as media for air pollution control systems: contaminant removal, applications and future research directions. Sci Total Environ 753:142249

Hale SE, Lehmann J, Rutherford D, Zimmerman AR, Bachmann RT, Shitumbanuma V, O'Toole A, Sundqvist KL, Arp HPH, Cornelissen G (2012) Quantifying the total and bioavailable polycyclic aromatic hydrocarbons and dioxins in biochars. Environ Sci Technol 46(5):2830–2838

Halsey G (1948) Physical adsorption on non-uniform surfaces. J Chem Phys 16(10):931–937

Harkins WD, Jura G (1944) The decrease (π) of free surface energy (γ) as a basis for the development of equations for adsorption isotherms; and the existence of two condensed phases in films on solids. J Chem Phys 12(3):112–113

Heidari A, Younesi H, Rashidi A, Ghoreyshi AA (2014) Evaluation of CO2 adsorption with eucalyptus wood based activated carbon modified by ammonia solution through heat treatment. Chem Eng J 254:503–513

Heo Y-J, Park S-J (2015) A role of steam activation on CO2 capture and separation of narrow microporous carbons produced from cellulose fibers. Energy 91:142–150

Hervy M, Pham Minh D, Gérente C, Weiss-Hortala E, Nzihou A, Villot A, Le Coq L (2018) H2S removal from syngas using wastes pyrolysis chars. Chem Eng J 334:2179–2189

Ho YS, McKay G (1999) Pseudo-second order model for sorption processes. Process Biochem 34(5):451–465

Hossain MK, Strezov V, Chan KY, Ziolkowski A, Nelson PF (2011) Influence of pyrolysis temperature on production and nutrient properties of wastewater sludge biochar. J Environ Manage 92(1):223–228

Ismadji S, Sudaryanto Y, Hartono SB, Setiawan LEK, Ayucitra A (2005) Activated carbon from char obtained from vacuum pyrolysis of teak sawdust: pore structure development and characterization. Biores Technol 96(12):1364–1369

JALON (2017) Zeolite | molecular sieve. https://www.molecular-sieve.cc/faq/molecular-sieve-adsorption-f.html, Accessed 29 May 2021

Kecili R, Hussain CM (2018) Chapter 4—mechanism of adsorption on nanomaterials. In: Hussain CM (ed) Nanomaterials in chromatography. Elsevier, pp 89–115

Khandaker T, Hossain MS, Dhar PK, Rahman MS, Hossain MA, Ahmed MB (2020) Efficacies of carbon-based adsorbents for carbon dioxide capture. Processes 8(6):654

Khuong DA, Nguyen HN, Tsubota T (2021a) CO 2 activation of bamboo residue after hydrothermal treatment and performance as an EDLC electrode. RSC Adv 11:9682–9692

Khuong DA, Nguyen HN, Tsubota T (2021b) Activated carbon produced from bamboo and solid residue by CO2 activation utilized as CO2 adsorbents. Biomass Bioenerg 148:106039

King R (2013) Biochar: a brief history and developing future. Mongabay Environ News. https://news.mongabay.com/2013/01/biochar-a-brief-history-and-developing-future/, Accessed 9 May 2021

Kodama H, Jaakkimainen M, Ducourneau R (1987) A multi-sample holder assembly for the quantasorb® surface analyzer. Canad J Soil Sci 67(3)

Lagergren S (1898) Zur Theorie der sogenannten Adsorption gelöster Stoffe Kungliga Svenska Vetenskapsakademiens. Handingar 24(4):1–39

Landers J, Gor GY, Neimark AV (2013) Density functional theory methods for characterization of porous materials. Colloids Surf, A 437:3–32

Langmuir I (1918) The adsorption of gases on plane surfaces of glass, mica and platinum. J Am Chem Soc 40(9):1361–1403

Machida T, Nakazawa T, Fujii Y, Aoki S, Watanabe O (1995) Increase in the atmospheric nitrous oxide concentration during the last 250 years. Geophys Res Lett—Geophys Res Lett 22:2921–2924

Madzaki H, KarimGhani WAWAB, Rebitanim NZ, Alias AB (2016) Carbon dioxide adsorption on sawdust biochar. Proc Eng 148:718–725

Manyà JJ, González B, Azuara M, Arner G (2018) Ultra-microporous adsorbents prepared from vine shoots-derived biochar with high CO2 uptake and CO2/N2 selectivity. Chem Eng J 345:631–639

Marsh H, Rodríguez-Reinoso F (2006) CHAPTER 4—Characterization of activated carbon. In: Marsh H, Rodríguez-Reinoso F (eds) Activated carbon. Elsevier Science Ltd, Oxford, pp 143–242

Menéndez-Díaz JA, Martín-Gullón I (2006) Chapter 1 types of carbon adsorbents and their production. In: Bandosz TJ (ed.) Interface science and technology. Elsevier, pp 1–47

Nsi E, Akpakpan A, Ukpong E, Akpabio U (2016) Preparation and characterization of activated carbon from hura crepitans linn seed shellspreparation and characterization of activated carbon from hura crepitans linn seed shells. Int J Eng Sci (IJES) 5:38–41

Oginni O, Singh K, Oporto G, Dawson-Andoh B, McDonald L, Sabolsky E (2019) Effect of one-step and two-step H3PO4 activation on activated carbon characteristics. Biores Technol Rep 8:100307

Freundlich H (1911) Kapillarchemie, Eine Darstellung der Chemie der Kolloide und verwandter Gebiete. Nature 85(2156):534–535

Petrovic B, Gorbounov M, Masoudi Soltani S (2021) Influence of surface modification on selective CO2 adsorption: a technical review on mechanisms and methods. Microporous Mesoporous Mater 312:110751

Prauchner MJ, Rodríguez-Reinoso F (2012) Chemical versus physical activation of coconut shell: a comparative study. Microporous Mesoporous Mater 152:163–171

Rittl TF, Oliveira DMS, Canisares LP, Sagrilo E, Butterbach-Bahl K, Dannenmann M, Cerri CEP (2021) High application rates of biochar to mitigate N2O emissions from a N-fertilized tropical soil under warming conditions. Front Environ Sci 8:611873

Robens E (1994) Some intriguing items in the history of adsorption. In: Rouquerol J, Rodríguez-Reinoso F, Sing KSW, Unger KK (eds) Studies in surface science and catalysis. Elsevier, pp 109–118

Robens E, Jayaweera SAA (2014) Early history of adsorption measurements. Adsorpt Sci Technol 32(6):425–442

Rodríguez-Reinoso F (2001) Activated carbon and adsorption. In: Buschow KHJ, Cahn RW, Flemings MC, Ilschner B, Kramer EJ, Mahajan S, Veyssière P (eds) Encyclopedia of materials: science and technology. Elsevier, Oxford, pp 22–34

Rouquerol F, Rouquerol J, Sing K (1999a) CHAPTER 1—Introduction. In: Rouquerol F, Rouquerol J, Sing K (eds) Adsorption by powders and porous solids. Academic Press, London, pp 1–26

Rouquerol F, Rouquerol J, Sing K (1999b) CHAPTER 2—Thermodynamics of adsorption at the gas–solid interface. In: Rouquerol F, Rouquerol J, Sing K (eds) Adsorption by powders and porous solids. Academic Press, London, pp 27–50

Rouquerol F, Rouquerol J, Sing KSW (2014) 2—Thermodynamics of adsorption at the gas/solid interface. In: Rouquerol F, Rouquerol J, Sing KSW, Llewellyn P, Maurin G (eds) Adsorption by powders and porous solids, 2nd edn. Academic Press, Oxford, pp 25–56

Sadasivam BY, Reddy KR (2014) Quantifying the effects of moisture content on transport and adsorption of methane through biochar in landfills. 191–200

Sadasivam BY, Reddy KR (2015) Adsorption and transport of methane in biochars derived from waste wood. Waste Manage 43:218–229

Sajjadi B, Chen W-Y, Egiebor NO (2019) A comprehensive review on physical activation of biochar for energy and environmental applications. Rev Chem Eng 35(6):735–776

Scholes C, Kentish S, Stevens G (2010) Carbon dioxide separation through polymeric membrane systems for flue gas applications. Recent Pat Chem Eng 1.

Seaton NA, Walton JPRB, Quirke N (1989) A new analysis method for the determination of the pore size distribution of porous carbons from nitrogen adsorption measurements. Carbon 27(6):853–861

Sethupathi S, Zhang M, Rajapaksha AU, Lee SR, Mohamad Nor N, Mohamed AR, Al-Wabel M, Lee SS, Ok YS (2017) Biochars as potential adsorbers of CH4, CO2 and H2S. Sustainability 9(1):121

Shang G, Shen G, Liu L, Chen Q, Xu Z (2013) Kinetics and mechanisms of hydrogen sulfide adsorption by biochars. Biores Technol 133:495–499

Shim T, Yoo J, Ryu C, Park Y-K, Jung J (2015) Effect of steam activation of biochar produced from a giant Miscanthus on copper sorption and toxicity. Biores Technol 197:85–90

Solaiman Z, Anawar HM (2015) Application of biochars for soil constraints: challenges and solutions. Pedosphere 25(5):631–638

Sadasivam BY, Reddy KR (2013) Study of methane adsorption by biochar in landfill cover. Paper presented in 106th annual conference & exhibition, air & watse management assocociation, USA, 1 June 2013

Temkin MI (1940) Kinetics of ammonia synthesis on promoted iron catalysts. Acta Physiochim URSS 12:327–356

Timur S, Ikizoglu E, Yanik J (2006) Preparation of activated carbons from oreganum stalks by chemical activation. Energy Fuels 20(6):2636–2641

Wang L, Wang Z, Li X, Yang Y (2020) Molecular dynamics mechanism of CH4 diffusion inhibition by low temperature in anthracite microcrystallites. ACS Omega 5(36):23420–23428

Weber WJ, Morris JC (1963) Kinetics of adsorption on carbon from solution. J Sanit Eng Div 89(2):31–59

Xiao F, Gámiz B, Pignatello JJ (2018) Adsorption and desorption of nitrous oxide by raw and thermally air-oxidized chars. Sci Total Environ 643:1436–1445

Yahia MB, Torkia YB, Knani S, Hachicha MA, Khalfaoui M, Lamine AB (2013) Models for type VI adsorption isotherms from a statistical mechanical formulation. Adsorpt Sci Technol 31(4):341–357

Zhdanov VP (2001) Adsorption–desorption kinetics and chemical potential of adsorbed and gas-phase particles. J Chem Phys 114(10):4746–4748

Zhelezova A, Cederlund H, Stenström J (2017) Effect of biochar amendment and ageing on adsorption and degradation of two herbicides. Water Air Soil Pollut 228(6):216

Zubbri NA, Mohamed AR, Kamiuchi N, Mohammadi M (2020) Enhancement of CO2 adsorption on biochar sorbent modified by metal incorporation. Environ Sci Pollut Res 27(11):11809–11829

Zulkurnai NZ, Ali UFM, Ibrahim N, Manan NSA (2017) Carbon dioxide (CO2) adsorption by activated carbon functionalized with deep eutectic solvent (DES). IOP Conf Ser: Mater Sci Eng 206:012001